environmental microbiology

Environmental Microbiology (2020) **00**(00), 00–00 doi:10.1111/1462-2920.15148

Trehalose-6-phosphate-mediated phenotypic change in *Acinetobacter baumannii*

Josephine Joy Hubloher,[1] Sabine Zeidler,[1] Pedro Lamosa,[2] Helena Santos,[2] Beate Averhoff[1] and Volker Müller[1]*

[1]*Department of Molecular Microbiology & Bioenergetics, Institute of Molecular Biosciences, Goethe-University Frankfurt am Main, Germany.*

[2]*Instituto de Tecnologia Química e Biológica António Xavier, Universidade Nova de Lisboa, Oeiras, Portugal.*

Summary

The stress protectant trehalose is synthesized in *Acinetobacter baumannii* from UPD-glucose and glucose-6-phosphase *via* the OtsA/OtsB pathway. Previous studies proved that deletion of *otsB* led to a decreased virulence, the inability to grow at 45°C and a slight reduction of growth at high salinities indicating that trehalose is the cause of these phenotypes. We have questioned this conclusion by producing Δ*otsA* and Δ*otsBA* mutants and studying their phenotypes. Only deletion of *otsB*, but not deletion of *otsA* or *otsBA*, led to growth impairments at high salt and high temperature. The intracellular concentrations of trehalose and trehalose-6-phosphate were measured by NMR or enzymatic assay. Interestingly, none of the mutants accumulated trehalose any more but the Δ*otsB* mutant with its defect in trehalose-6-phosphate phosphatase activity accumulated trehalose-6-phosphate. Moreover, expression of *otsA* in a Δ*otsB* background under conditions where trehalose synthesis is not induced led to growth inhibition and the accumulation of trehalose-6-phosphate. Our results demonstrate that trehalose-6-phosphate affects multiple physiological activities in *A. baumannii* ATCC 19606.

Introduction

Members of the genus *Acinetobacter* are Gram-negative rods thriving in diverse ecosystems and even extremophilic strains growing at high salinity and/or UV light are known (Albarracín *et al*., 2012; Kurth *et al*., 2015). Environmental strains are well known for their metabolic diversity and, in particular, for their ability to oxidize aromatic compounds by a specialized pathway, the ß-ketoadipate pathway (Stainer and Ornston, 1973). The biochemistry and regulation of this pathway have been well studied in *Acinetobacter baylyi* (Stainer and Ornston, 1973; Neidle and Ornston, 1986; Brzostowicz *et al*., 2003). Some *Acinetobacter* species such as *Acinetobacter baumannii* are opportunistic human pathogens, whose natural habitat is still unknown (Antunes *et al*., 2014). They have gained much attraction since the Iraq and Afghanistan war 2002–2004 when many soldiers were infected with *A. baumannii* (Centers for Disease Control and Prevention, 2004). Since then, *A. baumannii* has started a triumphal march and has become a major threat in health care institutions worldwide (Dijkshoorn *et al*., 2007; Averhoff, 2015). Over the last decade, infections with multidrug-resistant (MDR) *A. baumannii* have steadily increased (Dijkshoorn *et al*., 2007; Perez *et al*., 2007; Peleg *et al*., 2008) and, therefore, the World Health Organization has placed carbapenem-resistant *A. baumannii* on position 1 (together with carbapenem-resistant *Pseudomonas aeruginosa*, and carbapenem-resistant, ESBL-producing *Enterobacteriaceae*) at its 'critical' level in February 2017, to prioritize research and development efforts for new antimicrobial treatment (World Health Organization, 2017).

Unlike other pathogens, *A. baumannii* does not produce toxins (Peleg *et al*., 2008; Antunes *et al*., 2014; Harding *et al*., 2018). Instead, *A. baumannii* possesses virulence factors that confer adaptation to the human host. These virulence factors mediate cell adhesion and invasion, iron uptake, acquisition of multiple carbon and energy sources, capsule or biofilm formation (Farrugia *et al*., 2013; Stahl *et al*., 2015; Chapartegui-González *et al*., 2018; Ramirez *et al*., 2019; Runci *et al*., 2019; Singh *et al*., 2019; Weidensdorfer *et al*., 2019). Apart from the adaptation to the human host *A. baumannii* withstands dry conditions for a long time and is able to grow at high salt concentrations and high osmolarities in general (Zeidler *et al*., 2017; Chiang *et al*., 2018; Farrow *et al*., 2018; Zeidler *et al*., 2018; Zeidler and

Received 14 May, 2020; revised 22 June, 2020; accepted 29 June, 2020. *For correspondence. E-mail vmueller@bio.uni-frankfurt.de; Tel. (+49) 69 79829507; Fax. (+49) 69 79829306.

Müller, 2019b). The unravelling of the molecular basis of desiccation- and osmo-resistance has just begun. Life in high salt, high osmolarity and dry environments has a common feature: a low water activity of the environment (Vriezen *et al*., 2007; Zeidler and Müller, 2019a). Since biological membranes are permeable to water, water is pulled out of the cells at low water activities in the environment, cells shrink and die, if no countermeasures are taken (Roeßler and Müller, 2001; Bremer and Krämer, 2019). The action that *Acinetobacter* species such as *A. baumannii* or *A. baylyi* take is the accumulation of compatible solutes inside the cell (Sand *et al*., 2013; Zeidler *et al*., 2017; Zeidler *et al*., 2018). Compatible solutes such as glycine betaine or its precursor choline are taken up from the environment, or synthesized *de novo* such as glutamate or mannitol (Sand *et al*., 2013; Scholz *et al*., 2016; Zeidler *et al*., 2017; Zeidler *et al*., 2018). The pathways involved and their regulation has been reviewed recently (Zeidler and Müller, 2019a).

In addition to glutamate and mannitol, *A. baumannii* synthesizes trehalose as a response to salt and heat stress, albeit in very low amounts (Zeidler *et al*., 2017) and therefore, trehalose has been overlooked for some time. Trehalose is synthesized by *A. baumannii* by a two-step process. First, OtsA, a trehalose-6-phosphate synthase, condenses glucose-6-phosphate and UDP-glucose to trehalose-6-phosphate (Tre-6-P), which is dephosphorylated by OtsB, a trehalose-6-phosphate phosphatase to trehalose and inorganic phosphate (Zeidler *et al*., 2017). Expression of *otsB* is salt- and heat-stimulated and a Δ*otsB* mutant no longer accumulates trehalose and no longer grows at high temperatures (Zeidler *et al*., 2017). Growth at high salinities is marginally affected, which is consistent with the observation that trehalose is only a minor compatible solute. Trehalose is not only known to protect bacteria against osmotic stresses, but also it is a multifunctional molecule that protects bacteria against various stresses like desiccation, temperature stress and confers drug resistance (Welsh and Herbert, 1999; Elbein *et al*., 2003; Reina-Bueno *et al*., 2012; Lee *et al*., 2019). Most interestingly, a Δ*otsB* mutant is no longer able to infect *Galleria mellonella*, a moth model to study infection of eukaryotes by *A. baumannii* (Gebhardt *et al*., 2015). One of the obvious open questions was whether the lack of trehalose or a possible accumulation of Tre-6-P is the cause of the observed phenotypes. To address this important question, we have constructed a Δ*otsA* mutant and a Δ*otsB*/*otsA* double mutant and studied their phenotypes in comparison to the Δ*otsB* mutant.

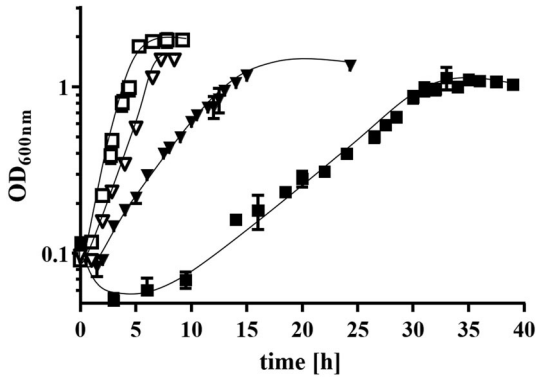

Fig 1. Effect of different carbon and energy sources and increasing NaCl concentrations on growth of *A. baumannii* ATCC 19606. Cells were grown in mineral medium either with succinate (squares) or arabinose (triangles) as sole carbon and energy source. The precultures were grown overnight in mineral medium with the same carbon and energy source and without addition of NaCl and used to inoculate fresh media without any additional osmolyte (open symbols) or with the addition of 500 mM NaCl (closed symbols). All cultivations were performed at 37°C. The standard error of the mean was calculated from three independent experiments.

Results

Intracellular trehalose concentrations are increased in arabinose-grown cells

Since the amount of trehalose produced during growth on succinate at 37°C was very small, we aimed to find a substrate leading to higher trehalose yields. Arabinose is a known carbon and energy source for *A. baumannii* ATCC 19606 and growth on succinate or arabinose in mineral medium was comparable (Fig. 1). At 500 mM NaCl, growth on arabinose was much faster than growth on succinate, nearly identical to growth in the absence of NaCl, indicating that arabinose-grown cells can cope better with high salinities than succinate-grown cells. Indeed, the intracellular concentration of trehalose increased up to 0.12 μmol mg^{-1} protein and was fourfold higher than in succinate-grown cells (0.03 μmol mg^{-1} protein in the late stationary phase). Moreover, even in the absence of additional NaCl, arabinose-grown cells produced trehalose, albeit in very small amounts and only in the late stationary phase (0.008 μmol mg^{-1} protein). We assume that cells grown on the sugar arabinose may have an energetic benefit over succinate-grown cells. This benefit seems to be used for trehalose synthesis in the late stationary phase.

Construction of Δ otsA *and* Δ otsBA *mutants*

Acinetobacter baumannii ATCC 19606 accumulates trehalose *via* the OtsAB pathway. As described previously deletion of *otsB* results in the inability to accumulate trehalose under osmotic stress and heat (Zeidler *et al*., 2017). To address the role of OtsA, a markerless

Δ*otsA* and Δ*otsA*/*otsB* double mutant was generated using the established insertion-duplication procedure (Stahl *et al*., 2015). Deletion of *otsA* or *otsBA* was confirmed by sequencing of the PCR product obtained with the primer pair *otsBA*_locus (Fig. 2).

A ΔotsB *mutant accumulates Tre-6-P and is impaired in growth at high salt and high temperature, whereas* ΔotsA *and* ΔotsBA *mutants do not exhibit these two phenotypes*

In previous experiments with cells grown on succinate at 37°C, little trehalose was produced upon osmotic upshift and a Δ*otsB* mutant growing at 500 mM NaCl had only a slightly reduced growth rate of 0.08 h^{-1} (td =8.3 h) compared to 0.13 h^{-1} of the wild type (td =5.2 h). However, the phenotype of the Δ*otsB* mutant was much more pronounced during growth on arabinose. Deletion of *otsB* caused a prolonged lag phase during the adaptation on mineral medium with arabinose as sole energy and carbon source and the addition of 300 mM NaCl largely impaired growth (Fig. 3). In contrast, the Δ*otsA* and the Δ*otsB*/*otsA* mutants had no growth phenoytpe, neither at low nor at high NaCl (Fig. 3). To complement the Δ*otsB* mutant, *otsB* was integrated into the genome by the use of a Rec_{AB}-recombineering system. In addition, upstream of *otsB* we inserted the putative *otsBA* promoter. The complemented strain Δ*otsB*_P_{otsBA}_*otsB* exhibited a growth rate at high salt comparable to the wild-type strain (Fig. 3). This provides evidence that the impaired growth rate of the Δ*otsB* mutant at high salt is due to the *otsB* deletion.

To determine trehalose and Tre-6-P concentrations, solutes were extracted from the cells with ethanol-chloroform, identified by NMR and quantified. As seen before, wild-type cells accumulated trehalose, whereas neither the Δ*otsB* nor the Δ*otsA* and Δ*otsB*/*otsA* mutants did (Fig. 4A). The Δ*otsB* mutant accumulated Tre-6-P, however the Δ*otsA* or Δ*otsB*/*otsA* double mutant did not (Fig. 4B). Notably, the Tre-6-P concentration in the Δ*otsB* mutant was 25-fold higher than the trehalose concentration in wild-type cells. When the Δ*otsB* mutant was complemented with *otsB* trehalose was again accumulated (Fig. 4C) and Tre-6-P accumulation was nearly abolished (Fig. 4D). If the impaired growth phenotype of the Δ*otsB* mutant at high salt is caused by accumulation of Tre-6-P, breakdown of Tre-6-P by another enzyme should restore the wild type phenotype. To address this question, *treC*, encoding a trehalose-6-phosphate hydrolase from *Escherichia coli* (Rimmele and Boos, 1994), was cloned into the Δ*otsB* mutant by using the Rec_{AB}-recombineering system. The Δ*otsB* + P_{otsBA}_*treC* mutant grew like the wild type strain on arabinose (Fig. 3) and Tre-6-P was no longer

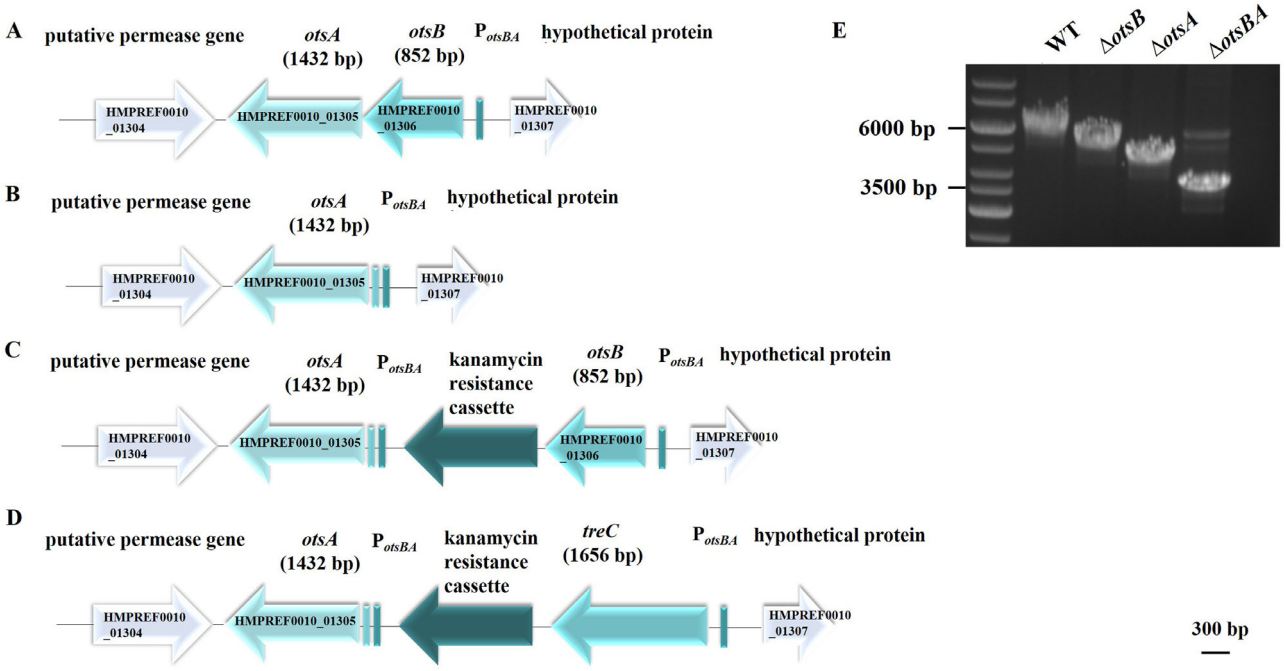

Fig 2. Genetic organization of the *otsBA* locus in *A. baumannii* ATCC 19606 (A) the Δ*otsB* mutant (B) and the strains Δ*otsB* + P_{otsBA}_*otsB* (C) and Δ*otsB* + P_{otsBA}_*trec* (D). The *otsBA* locus was amplified in *A. baumannii* 19606 and the Δ*ots* mutants *via* PCR using the primer pair *otsBA*_locus (E).

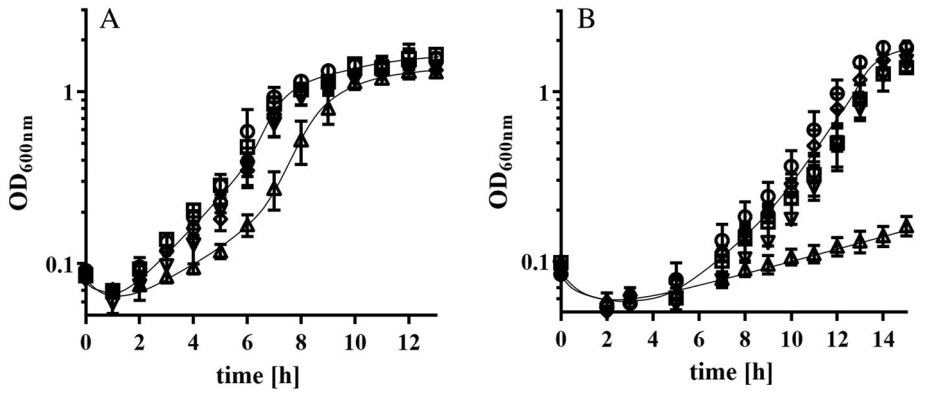

Fig 3. Effect of deletion of the *ots* genes in *A. baumannii* ATCC 19606 on growth in mineral medium with arabinose and increasing NaCl concentrations. *A. baumannii* ATCC19606 (○), Δ*otsA* (□), Δ*otsBA* (▽), Δ*otsB* (△), Δ*otsB*_P_{otsBA}_*otsB* (◇) and Δ*otsB*_P_{otsBA}_*treC* (○) were inoculated from a preculture grown in mineral medium with succinate into mineral medium with arabinose without (A) or with the addition of 300 mM NaCl (B). All cultivations were performed at 37°C. The standard error of the mean was calculated from three independent experiments.

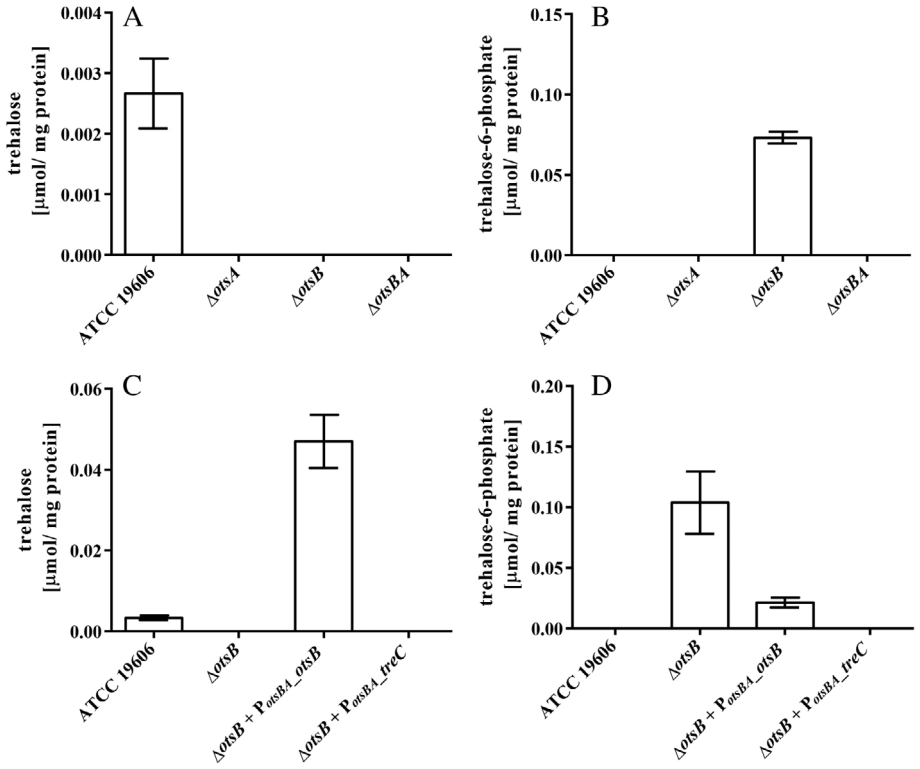

Fig 4. Intracellular accumulation of trehalose and Tre-6-P in *A. baumannii* ATCC 19606 and the *ots* strains during growth in mineral medium with arabinose and salt stress. *A. baumannii* ATCC 19606, the Δ*ots* mutants, Δ*otsB*_P_{otsBA}_*otsB* and Δ*otsB*_P_{otsBA}_*treC* were grown overnight in mineral medium with succinate as sole carbon and energy source. The precultures were used to inoculate fresh mineral medium with arabinose as sole energy and carbon source and 300 mM NaCl. After 10 h of growth the intracellular trehalose and Tre-6-P concentration of the strains was analysed *via* NMR (A + B) or with an enzymatic assay (C + D). The standard deviation was calculated from three independent experiments.

accumulated (Fig. 4D). This suggests that indeed the growth phenotype of the Δ*otsB* mutant was due to the accumulation of Tre-6-P.

As originally described, the Δ*otsB* mutant did not grow at 45°C in mineral medium with succinate (Zeidler *et al*., 2017); however, the Δ*otsA* and Δ*otsB*/*otsA* mutants did (Fig. 5). The same holds true for the strains Δ*otsB*_P_{otsBA}_*otsB* and Δ*otsB*_P_{otsBA}_*treC* (Fig. 5). The wild type accumulated only little trehalose at 45°C (Fig. 6A), but again Tre-6-P accumulated in the Δ*otsB* mutant to levels comparable to cells grown with arabinose at high NaCl (Figs. 4B and 6B). Tre-6-P accumulation at 45°C was strongly reduced in the Δ*otsB*_P_{otsBA}_*otsB* strain and the strain Δ*otsB*_P_{otsBA}_*treC* did not accumulate Tre-6-P at all (Fig. 6B). As expected, complementation with *otsB* restored the ability to synthesize trehalose while integration of *treC* abolished Tre-6-P accumulation but did not restore trehalose accumulation (Fig. 6A). In addition, these experiments clearly demonstrate that the Δ*otsB* mutant accumulates Tre-6-P and provides evidence that the impaired growth phenotype of the Δ*otsB* mutant at high salt or high temperature is not due to the lack of trehalose but due to the accumulation of Tre-6-P.

Overexpression of otsA *leads to accumulation of Tre-6-P and growth inhibition*

The data presented so far led to the conclusion that accumulation of Tre-6-P causes growth inhibition. To further underline this conclusion, we generated strains that conditionally express the *ots* genes. We assumed that expression of *otsA* should result in Tre-6-P production. Therefore, the Δ*otsB* mutant was transformed with the plasmids pVRL2_P_{ara}_*otsA*, pVRL2_P_{ara}_*otsB* and pVRL2_P_{ara}_*otsBA*. These plasmids encode the *ots* genes (*otsA*, *otsB* or *otsBA*) under transcriptional control of an arabinose-inducible promoter. This resulted in three strains producing OtsA, OtsB or OtsBA upon induction by arabinose. The strains were grown overnight in mineral medium with succinate at 37°C and low NaCl to avoid expression of *ots* genes. These precultures were then used to inoculate mineral medium containing 1, 2 or 4% arabinose. Growth of the Δ*otsB* mutant was only marginally affected under these conditions, since the inducer of gene expression (heat or high NaCl) was lacking (Fig. 3A). However, the strains expressing *otsA* from the arabinose inducible promoter had a pronounced growth phenotype. At 1% the growth rate was 0.24 h^{-1} compared with 0.58 h^{-1} for the wild type grown on arabinose at low NaCl. Higher arabinose concentrations inhibited growth even more (μ = 0.034 h^{-1} at 2% and μ = 0.024 h^{-1} at 4%) (Fig. 7). Expression of *otsA* in the Δ*otsB* mutant led to the synthesis of Tre-6-P and the level of Tre-6-P increased with the arabinose concentration. There was no Tre-6-P accumulated in the strains Δ*otsB* + pVRL2_P_{ara}_*otsB* and Δ*otsB* + pVRL2_P_{ara}_*otsBA* expressing *otsB* or *otsBA* upon induction by arabinose (Fig. 8). These data are in line with our conclusion that accumulation of Tre-6-P leads to growth inhibition and is the cause of the phenotype of the Δ*otsB* mutant.

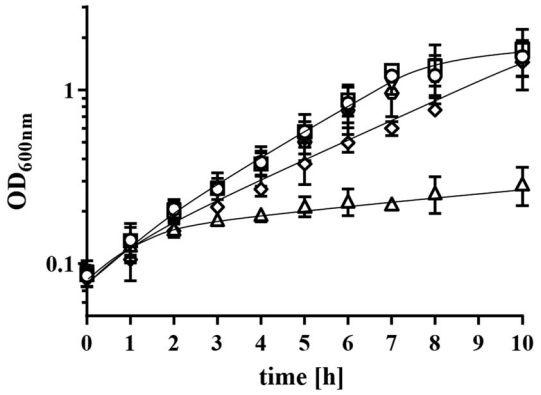

Fig 5. Effect of deletion of *ots* genes on growth of *A. baumannii* ATCC 19606 at 45°C. *A. baumannii* ATCC 19606 (○), Δ*otsA* (□), Δ*otsBA* (▽), Δ*otsB* (△), Δ*otsB*_P_{otsBA}_*otsB* (◇) and Δ*otsB* _P_{otsBA}_*treC* (□) were grown overnight in mineral medium with succinate as sole energy and carbon source at 37°C. The precultures were used to inoculate prewarmed (45°C) mineral medium with succinate as sole energy and carbon source, cells were grown at 45°C. The standard error of the mean was calculated from three independent experiments.

Discussion

In this study, we have provided compelling evidence that the growth-impaired phenotype at high temperature or high salt of the Δ*otsB* mutant of *A. baumannii* ATCC 19606 is not caused by the lack of trehalose accumulation but instead by the accumulation of Tre-6-P. For a long time, Tre-6-P was thought to only be an intermediate of a metabolic pathway without any further physiological implications. However, genetic studies revealed that Tre-6-P plays a regulatory role in plants (Figueroa and Lunn, 2016) as well as in fungi and nematodes (Borgia *et al*., 1996; Kormish and McGhee, 2005; Deroover *et al*., 2016; Thammahong *et al*., 2017). Furthermore, there is a report of Tre-6-P-mediated regulation in bacteria, in the human pathogen *Mycobacterium tuberculosis* (Korte and Alber, 2016). Regulation by Tre-6-P can occur either through the absence of Tre-6-P or its hyperaccumulation. In plants and yeast Tre-6-P is

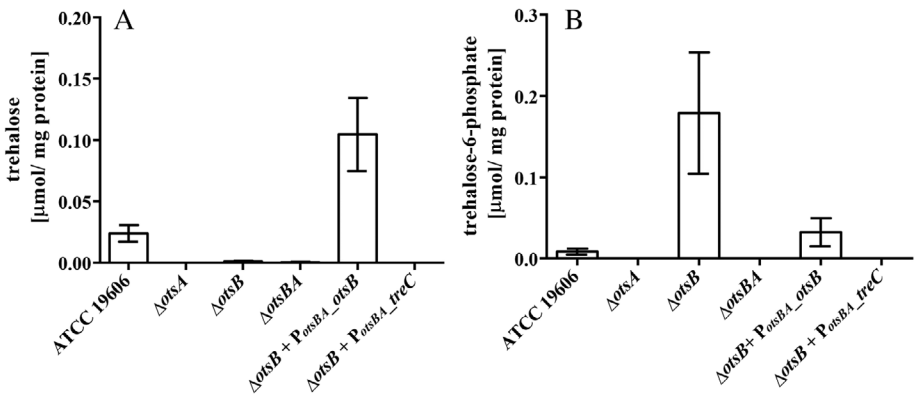

Fig 6. Intracellular trehalose and Tre-6-P concentration in *A. baumannii* ATCC 19606 and Δ*ots* mutants during growth in mineral medium at 45°C. *A. baumannii* ATCC 19606 and the Δ*ots* mutants were grown in mineral medium with succinate as sole carbon and energy source at 45°C. After 8 h of growth, the intracellular trehalose (A) and Tre-6-P (B) concentration of the strains was analysed with an enzymatic assay. The standard deviation was calculated from three independent experiments.

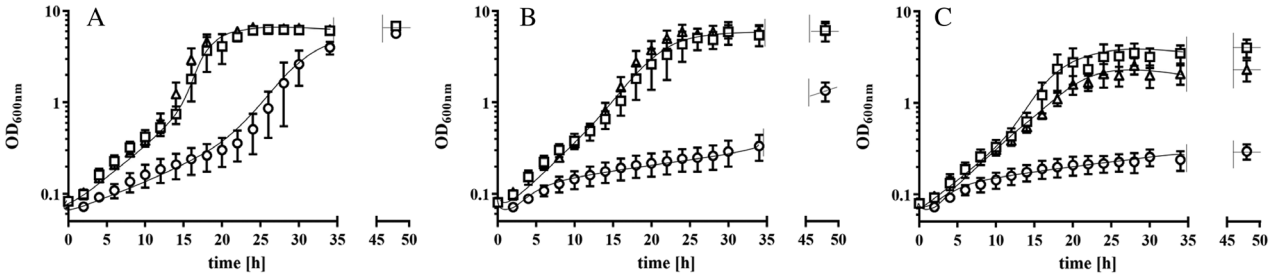

Fig 7. Expression of *otsA* impairs growth of *A. baumannii* Δ*otsB*. The Δ*otsB* mutants were transformed with the pVRL2-plasmid encoding *otsA* (○), *otsB* (○), or *otsBA* (△) under the transcriptional control of an arabinose-inducible promoter. Strains were grown at 37°C in the presence of 1% (A), 2% (B) or 4% (C) arabinose as sole carbon and energy source and inducer. The precultures were grown in mineral medium at 37°C with succinate to avoid expression of the *ots* genes. The standard error of the mean was calculated from three independent experiments.

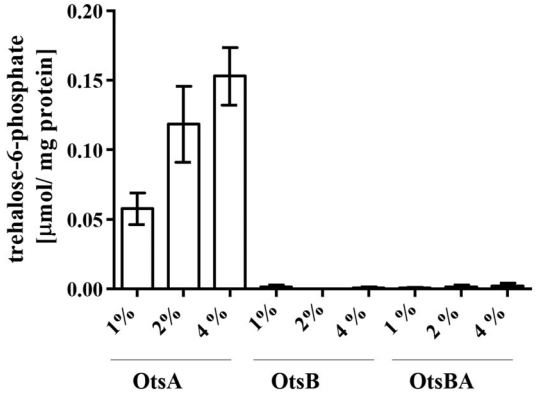

Fig 8. Intracellular accumulation of Tre-6-P in *A. baumannii* Δ*otsB* producing OtsA. The Δ*otsB* mutants were transformed with plasmid pVRL2 coding for *otsA* (○), *otsB* (△), or *otsBA* (△) under an arabinose-inducible promoter. Strains were grown at 37°C in the presence of 1, 2 or 4% arabinose as sole carbon and energy source and inducer. After 24 h, cells were harvested and solutes were analysed by enzymatic assays. The precultures were grown in mineral medium with succinate to avoid expression of the *ots* genes. The standard deviation was calculated from three independent experiments.

thought to be a signal molecule and a global regulator during development and sugar metabolism (Deroover *et al*., 2016; Figueroa and Lunn, 2016). *Arabidopsis thaliana*, for example, uses Tre-6-P to sense the availability of sucrose within the cell (Lunn *et al*., 2006). Deletion of the trehalose-6-phosphate synthase gene – and thus depletion of Tre-6-P – causes dramatic effects and interferes with growth and development (Zaragoza *et al*., 1998; van Vaeck *et al*., 2001; Eastmond *et al*., 2002; Gómez *et al*., 2006; Figueroa and Lunn, 2016; Thammahong *et al*., 2017; Vicente *et al*., 2018). In *A. baumannii* ATCC 19606, this is obviously different. We could not observe any growth defects of the Δ*otsA* or Δ*otsBA* mutant – both lacking the ability to synthesize Tre-6-P - providing evidence that Tre-6-P is not used as an essential signalling molecule during growth and development in *A. baumannii* ATCC 19606 or at least not under the tested conditions. In contrast, hyperaccumulation of Tre-6-P causes growth defects in *A. baumannii* ATCC 19606. A very similar observation was made in fungi. Deletion of the trehalose-6-phosphate phosphatase genes in *Saccharomyces cerevisiae* and *Aspergillus nidulans* caused a heat shock-dependent accumulation of Tre-6-P which was accompanied with growth inhibition (Piper and Lockheart, 1988; Borgia *et al*., 1996). Homozygote deletion of the two Tre-6-P phosphatase genes (Δ*tps2*Δ*tps2*) in *Candida albicans* also caused a heat sensitive phenotype and sensitivity against oxidative stress (Martínez-Esparza *et al*., 2009) and it was postulated that the heat sensitive phenotype was caused by Tre-6-P accumulation (Martínez-Esparza *et al*., 2009). Most of these studies argue for a growth inhibition due to Tre-6-P toxicity alone. This is also reported for *M. tuberculosis*, where the Tre-6-P phosphatase gene (*otsB2*) is essential and already very low amounts of Tre-6-P are highly toxic (Korte and Alber, 2016). In contrast, disruption of the Tre-6-P phosphatase gene (*orlA*) in *A. nidulans* causes Tre-6-P accumulation already at low temperature while growth was only inhibited at elevated temperatures (42°C) (Borgia *et al*., 1996). These findings pointed out that at least in the case of *A. nidulans* a simple toxicity of Tre-6-P cannot explain the temperature-dependent phenotype of the mutant. A similar observation was made in *A. baumannii* ATCC 19606 upon osmotic stress with regard to the carbon and energy source. Deletion of *otsB* caused no effect on growth in mineral medium with succinate and the addition of high amounts of sodium chloride (500 mM) caused only slight reduction of growth in comparison to the wild type (Zeidler *et al*., 2017). In contrast, the Δ*otsB* mutant was slightly impaired during growth on mineral medium with arabinose and the addition of sodium chloride (300 mM) abolished growth. These differences can be explained by a toxic effect of Tre-6-P that is dependent on the presence of special interaction partners, for example, enzymes that are involved in arabinose degradation.

The molecular mechanism behind Tre-6-P regulations is poorly understood. In *M. tuberculosis*, gene expression is strongly changed upon Tre-6-P accumulation. Silencing of *otsB2* in *M. tuberculosis* resulted in Tre-6-P accumulation and global changes in expression (877 upregualted and 37 downregulated genes) (Korte and Alber, 2016). Accumulation of the toxic sugar phosphate maltose-1-phosphate (Mal-1-P) in *M. tuberculosis* caused by deletion of the maltosyltransferase gene (*glgE*) was also associated with alterations in gene expression (Kalscheuer *et al*., 2010). Surprisingly, the overlap in alterations of gene expression dependent on Tre-6-P or Mal-1-P was small and restricted to upregulation of only a few genes involved in arginine synthesis and DNA damage-inducible genes (Kalscheuer *et al*., 2010; Korte and Alber, 2016). This comparison provides evidence that alterations in gene expression caused by Tre-6-P are quite specific (Korte and Alber, 2016).

However, there are also reports of Tre-6-P interaction with enzymes that are not involved in gene expression. The major hexokinase from *S. cerevisiae* is reported to be competitively inhibited by Tre-6-P *in vitro*. Even though *A. baumannii* ATCC 19606 does not encode a hexokinase a comparable effect could also be possible. Inhibition of enzymes that convert glucose-6-P or derivatives could also cause growth inhibition and could explain differences during growth on different carbon and energy sources.

In the human pathogen, *Aspergillus fumigatus* deletion of the Tre-6-P phosphatase gene abolished virulence (Puttikamonkul *et al*., 2010). Up to now the only studies that revealed an effect of trehalose genes on infection by *A. baumannii* AB5075 where those of Gebhardt *et al*. (2015). They observed that *otsB* belongs to the genes that are required for growth in *G. mellonella* larvae and that deletion of *otsB* results in an avirulent phenotype in *G. mellonella*. Interestingly, *otsA* did not belong to the genes that are required for growth in *G. mellonella* larvae (Gebhardt *et al*., 2015), arguing for a role of Tre-6-P in infection. Unfortunately, no infection studies with an *otsA* mutant were performed so far and the effect of Tre-6-P and trehalose during infection has to be studied in further experiments.

Table 1. Bacterial strains used in this study.

Strain	References
Escherichia coli DH5α	Invitrogen™, USA
Escherichia coli K12	Invitrogen™, USA
Acinetobacter baumannii ATCC 19606	ATCC, USA
Acinetobacter baumannii ATCC 19606 Δ*otsB*	(Zeidler *et al*., 2017)
Acinetobacter baumannii ATCC 19606 Δ*otsA*	This study
Acinetobacter baumannii ATCC 19606 Δ*otsBA*	This study
Acinetobacter baumannii ATCC 19606 Δ*otsB* + *PAT04*	This study
Acinetobacter baumannii ATCC 19606 Δ*otsB*_P_{otsBA}_*otsB*	This study
Acinetobacter baumannii ATCC 19606 Δ*otsB*_P_{otsBA}_*treC*	This study
Acinetobacter baumannii ATCC 19606 Δ*otsB* + pVRL2_P_{ara}_*otsA*	This study
Acinetobacter baumannii ATCC 19606 Δ*otsB* + pVRL2_P_{ara}_*otsB*	This study
Acinetobacter baumannii ATCC 19606 Δ*otsB* + pVRL2_P_{ara}_*otsBA*	This study

Experimental procedures

Bacterial strain and culture conditions

Bacterial strains used in this study are listed in Table 1. Bacteria were either grown in LB-media (Bertani, 1951) or in phosphate-buffered mineral medium (Zeidler *et al*., 2017) at 37°C or 45°C as specified in the experiments. Succinate or arabinose (20 mM each) was added as sole carbon and energy source. Growth experiments were performed in 500 ml Erlenmeyer flasks filled with 100 ml medium. Sodium chloride was added as indicated. Overnight cultures were then used to inoculate fresh media to an initial OD_{600nm} of 0.1. Growth was monitored photometrically by measuring the optical density at 600 nm. The *ots* expression strains were grown in presence of 100 μg ml^{-1} gentamicin.

Markerless mutagenesis

Markerless deletion of *otsA* (HMPREF0010_01305) or *otsBA* (HMPREF0010_01305 + HMPREF0010_01306) was performed using a *sacB*/*kanR* cassette as described before (Stahl *et al*., 2015). A 1500 bp DNA fragment spanning the region upstream the gene of interest and a 1500 bp fragment downstream of the gene of interest was amplified *via* PCR and cloned into pBIISK_*sacB_kanR* vector using Gibson assembly, according to the instructions of the manufacturer (Gibson Assembly Master Mix, New England Biolabs, Ipswich, MA, USA) (primers used are listed in the Supporting Information Table S1). The resulting recombinant plasmids were used to transform *A. baumannii* ATCC 19606 via electroporation (2.5 kV, 200 Ω and 25 μF). Transformants were selected on LB agar (1.8%) containing 50 μg ml^{-1} kanamycin. Counterselection was achieved by growing the strains in LB + 10% sucrose. Clones were screened for the loss of kanamycin resistance and deletion mutants were verified *via* PCR. The resulting PCR products were sequenced.

Generating the inserts for Rec_{AB}-mediated gene editing

Insertion of *otsB* or *treC* into the genome of the Δ*otsB* mutant was done in *cis* using the Rec_{AB}-recombineering system (Tucker *et al*., 2014). Therefore, two recombinant plasmids pBIISK_up_P_{otsBA}_*otsB_kan*^{R}_down and pBIISK_updo_P_{otsBA}_*treC_kan*^{R}_*down* were generated.

To generate pBIISK_updo_P_{otsBA}_*otsB_kan*^{R}, we amplified *otsB* and 338 bp preceding to *otsB* start codon (coding for the native promoter P_{otsBA}) from the genome of *A. baumannii* ATCC 19606 using the primer pair *otsB*_inkl_upstream. A kanamycin resistant marker was amplified from the plasmid pKD4 with the primer pair Kan_comp_fw. The 300 bp flanking the distinct insertion site (393 bp upstream of *otsA*) for recombineering were amplified from the genome of *A. baumannii* ATCC 19606 using the primer pairs Upstream_comp and Downstream_comp. The resulting PCR products were cloned into the vector pBIISK using Gibson assembly (Gibson Assembly Master Mix, New England Biolabs, Ipswich, MA, USA) resulting in the plasmid pBIISK_up_P_{otsBA}_*otsB_kan*^{R}_*down*.

To generate pBIISK_updo_P_{otsBA}_*treC_kan*^{R}_*down*, we amplified the plasmid pBIISK_updo_P_{otsBA}_*otsB_kan*^{R} without *otsB* using the primer pair pBIISK_P_{otsB}_*otsB*. *TreC* was amplified from genomic DNA from *E. coli* K12 using the primer pair *treC*. The resulting fragments were assembled using Gibson assembly (Gibson Assembly Master Mix, New England Biolabs) resulting in the plasmid pBIISK_up_P_{otsBA}_*treC_kan*^{R}_down.

The two recombinant plasmids pBIISK_up_P_{otsBA}_*otsB_kan*^{R}_down and pBIISK_up_P_{otsBA}_*treC_kan*^{R}_down were used as templates in a PCR using the primer pair Linear_PCR_fragment. The PCR fragments (P_{otsBA}_*otsB_kan*^{R} or P_{otsBA}_*treC_kan*^{R}) harbouring the *otsBA* promoter, *otsB* (or *treC*) and the kanamycin-cassette in a row – flanked by 125 bp upstream and downstream of the insertion region (393 bp upstream of *otsA*). The PCR fragments were then recombined into the genome of *A. baumannii* Δ*otsB* using the Rec_{AB}-system.

Rec_{AB}-mediated recombineering for gene editing

We used recombineering as genetic tool not for gene deletion as originally described (Tucker *et al*., 2014) but for gene insertion. To this end, we inserted P_{otsBA}_*otsB_kan*^{R} (or P_{otsBA}_*treC_kan*^{R}) into the genome of the Δ*otsB* mutant. First, we transformed the Δ*otsB* mutant with the pAT04_*Rec_{AB}* plasmid *via* electroporation (2.5 kV, 200 Ω and 25 μF) following the selection on LB agar containing 30 μg ml^{-1} tetracycline. The resulting strain Δ*otsB* + pAT04_*Rec_{AB}* is capable to facilitate recombineering. Recombineering was done according to Tucker *et al*. (2014). Briefly, 5 μg of either P_{otsBA}_*otsB_kan*^{R} or P_{otsBA}_*treC_kan*^{R} were transformed in the Rec_{AB} producing Δ*ostB* mutant *via* electroporation (2.5 kV, 200 Ω and 25 μF). Transformants were selected on LB agar containing kanamycin (7.5, 10 or 15 μg ml^{-1}). Integration of the PCR fragments was verified *via* PCR.

Generation of ots *expressing strains*

For the generation of *ots* expression strains, we used the Δ*otsB* mutant as parental strain and the *E. coli*/*Acinetobacter* shuttle plasmids pVRL2 (Lucidi *et al*., 2018) as backbone for the expression plasmids. Plasmids were designed according to Lucidi *et al*. (2018) with slight modifications. Briefly, *otsA*, *otsB* or *otsBA* were amplified *via* PCR from the genome of *A. baumannii* ATCC 19606. The resulting PCR products were cloned into the *SalI* and *SacI* restriction sites of pVRL2 (primers are listed in the Supporting Information Table S1). The resulting plasmids harbour either *otsA*, *otsB* or *otsBA* under the control of an arabinose-inducible promoter. The plasmids were verified by DNA sequencing. To generate the expression strains, *A. baumannii* Δ*otsB* was transformed with the recombinant pVRL2 plasmids *via* electroporation (2.5 kV, 200 Ω and 25 μF) following a selection of transformants on LB agar with 100 μg ml^{-1} gentamycin. The resulting expression strains Δ*otsB* + pVRL2_P_{ara}_*otsA*, Δ*otsB* + pVRL2_P_{ara}_*otsBA* and Δ*otsB* + pVRL2_P_{ara}_*otsB* were grown overnight in mineral medium with succinate, 100 μg ml^{-1} gentamycin and in the absence of arabinose. For expression studies, the overnight cultures were transferred in mineral medium with 1, 2 or 4% arabinose as sole carbon source and inducer.

NMR analyses

For NMR analyses, precultures were grown overnight at 37°C in mineral medium with succinate as carbon source. The precultures were used to inoculate mineral medium containing 20 mM arabinose as carbon source and 300 mM NaCl. Cells were grown at 37°C in 500 ml of the medium filled in 2 l erlenmeyer flasks. A total cell culture volume of 1.5 l was harvested in the case of *A. baumannii* ATCC 19606, Δ*otsA* and Δ*otsBA* mutant. In case of the Δ*otsB* mutant, 4.5 l of cell culture was harvested (4700 rpm, 4°C, 20 min) 10 h after inoculation. To generate a low phosphate background for NMR analyses, cells were washed two times with 300 mM NaCl (50 ml). Cell pellets were frozen in liquid nitrogen, lyophilized and stored at −65°C. Solutes were extracted using an ethanol-based extraction as previously described (Martins and Santos, 1995; Sand *et al*., 2011; Zeidler *et al*., 2017). ^{1}H-NMR spectra were acquired on a Bruker Avance III 800 spectrometer (Bruker, Rheinstetten,

Germany) working at a proton operating frequency of 800.33 MHz, equipped with a three channel 5 mm inverse detection probe head with pulse-field gradients at 25°C. A 1.5 s soft pulse before the excitation pulse was applied to pre-saturate the water signal. Spectra were acquired under fully relaxed conditions (flip angle 60°; repetition delay of 60 s) so that the area of the NMR signals was proportional to the amount of the different protons in the sample. For quantification purposes, formate was added as an internal concentration standard. To firmly assign the signals in the proton spectrum a ^{1}H-^{13}C correlation spectrum of a representative sample was also acquired. The ^{1}H-^{13}C heteronuclear single quantum coherence spectrum (HSQC) was acquired collecting 1024 ($t2$) × 256($t1$) data points, with a delay of 3.5 ms for the evolution of $^{1}J_{CH}$, using a composite adiabatic pulse sequence for proton decoupling and pulse field gradients for sensitivity enhancement (Schleucher *et al*., 1994). Protein content was determined using the BCA™ Protein Assay Kit (Pierce, Rockford, IL) after cell lysis by sonication.

Quantification of trehalose and Tre-6-P using enzymatic assays

Solutes were extracted as described before (Zeidler *et al*., 2017) and the pellet was dissolved in 212.5 µl H_2O. For quantification of trehalose and Tre-6-P, samples were divided into two portions, with a total volume of 85 µl each. To both samples 10 µl 10× FastAP Buffer (Thermo Fisher Scientific, Waltham, MA, USA) was added. In addition, 5 µl of H_2O was added to sample 1 for quantification of trehalose. The other part of the sample was treated with 5 µl FastAP (alkaline phosphatase; Thermo Fisher Scientific) for dephosphorylation of Tre-6-P. Both samples were incubated for 2 h at 37°C for complete dephosphorylation. The trehalose content of sample 1 and 2 was quantified with the trehalose assay kit 'K-TREH' (Megazyme, Bray, Ireland). Sample 1 reflects the amount of trehalose of the cell. Sample 2 reflects the trehalose and Tre-6-P amount of the cells. The subtraction of sample 1 from sample 2 gives the amount of Tre-6-P in the cells. The enzyme based dephosphorylation assay and quantification of Tre-6-P using NMR led to the same results.

Acknowledgements

The authors are indebted to the Deutsche Forschungsgemeinschaft for financial support through DFG Research Unit FOR 2251, to the Project LISBOA-01-0145-FEDER-007660 funded by FEDER through COMPETE2020 – POCI and by national funds through Fundação para a Ciência e a Tecnologia. The NMR data were acquired at CERMAX with equipment funded by Fundação para a Ciência e a Tecnologia, project AAC 01/SAICT/2016. Sara Rebelo is acknowledged for technical assistance.

References

Albarracín, V.H., Pathak, G.P., Douki, T., Cadet, J., Borsarelli, C.D., Gärtner, W., and Farias, M.E. (2012) Extremophilic *Acinetobacter* strains from high-altitude lakes in Argentinean Puna: remarkable UV-B resistance and efficient DNA damage repair. *Orig Life Evol Biosph* **42**: 201–221.

Antunes, L.C.S., Visca, P., and Towner, K.J. (2014) *Acinetobacter baumannii*: evolution of a global pathogen. *Pathog Dis* **71**: 292–301.

Averhoff, B. (2015) *Acinetobacter baumannii* - understanding and fighting a new emerging pathogen. *Environ Microbiol Rep* **7**: 6–8.

Bertani, G. (1951) Studies on lysogenesis. I The mode of phage liberation by lysogenic *Escherichia coli*. *J Bacteriol* **62**: 293–300.

Borgia, P.T., Miao, Y., and Dodge, C.L. (1996) The *orlA* gene from *Aspergillus nidulans* encodes a trehalose-6-phosphate phosphatase necessary for normal growth and chitin synthesis at elevated temperatures. *Mol Microbiol* **20**: 1287–1296.

Bremer, E., and Krämer, R. (2019) Responses of microorganisms to osmotic stress. *Annu Rev Microbiol* **73**: 313–334.

Brzostowicz, P.C., Reams, A.B., Clark, T.J., and Neidle, E.L. (2003) Transcriptional cross-regulation of the catechol and protocatechuate branches of the beta-ketoadipate pathway contributes to carbon source-dependent expression of the *Acinetobacter sp*. strain ADP1 *pobA* gene. *Appl Environ Microbiol* **69**: 1598–1606.

Centers for Disease Control and Prevention. (2004) *Acinetobacter baumannii* infections among patients at military medical facilities treating injured U.S. service members, 2002-2004. *MMWR Morb Mortal Wkly Rep* **53**: 1063–1066.

Chapartegui-González, I., Lázaro-Díez, M., Bravo, Z., Navas, J., Icardo, J.M., and Ramos-Vivas, J. (2018) *Acinetobacter baumannii* maintains its virulence after long-time starvation. *PLoS One* **13**: e0201961.

Chiang, S.R., Jung, F., Tang, H.J., Chen, C.H., Chen, C.C., Chou, H.Y., and Chuang, Y.C. (2018) Desiccation and ethanol resistances of multidrug resistant *Acinetobacter baumannii* embedded in biofilm: the favorable antiseptic efficacy of combination chlorhexidine gluconate and ethanol. *J Microbiol Immunol Infect* **51**: 770–777.

Deroover, S., Ghillebert, R., Broeckx, T., Winderickx, J., and Rolland, F. (2016) Trehalose-6-phosphate synthesis controls yeast gluconeogenesis downstream and independent of SNF1. *FEMS Yeast Res* **16**: fow036.

Dijkshoorn, L., Nemec, A., and Seifert, H. (2007) An increasing threat in hospitals: multidrug-resistant *Acinetobacter baumannii*. *Nat Rev Microbiol* **5**: 939–951.

Eastmond, P.J., van Dijken, A.J., Spielman, M., Kerr, A., Tissier, A.F., Dickinson, H.G., *et al*. (2002) Trehalose-6-phosphate synthase 1, which catalyses the first step in trehalose synthesis, is essential for *Arabidopsis* embryo maturation. *Plant J* **29**: 225–235.

Elbein, A.D., Pan, Y.T., Pastuszak, I., and Carroll, D. (2003) New insights on trehalose: a multifunctional molecule. *Glycobiology* **13**: 17R–27R.

Farrow, J.M., III, Wells, G., and Pesci, E.C. (2018) Desiccation tolerance in *Acinetobacter baumannii* is mediated by the two-component response regulator BfmR. *PLoS One* **13**: e0205638–e0205638.

Farrugia, D.N., Elbourne, L.D.H., Hassan, K.A., Eijkelkamp, B.A., Tetu, S.G., Brown, M.H., *et al*. (2013) The complete genome and phenome of a community-acquired *Acinetobacter baumannii*. *PLoS One* **8**: e58628.

Figueroa, C.M., and Lunn, J.E. (2016) A tale of two sugars: trehalose 6-phosphate and sucrose. *Plant Physiol* **172**: 7–27.

Gebhardt, M.J., Gallagher, L.A., Jacobson, R.K., Usacheva, E.A., Peterson, L.R., Zurawski, D.V., and Shuman, H.A. (2015) Joint transcriptional control of virulence and resistance to antibiotic and environmental stress in *Acinetobacter baumannii*. *MBio* **6**: e01660–e01615.

Gómez, L.D., Baud, S., Gilday, A., Li, Y., and Graham, I.A. (2006) Delayed embryo development in the *Arabidopsis* trehalose-6-phosphate synthase 1 mutant is associated with altered cell wall structure, decreased cell division and starch accumulation. *Plant J* **46**: 69–84.

Harding, C.M., Hennon, S.W., and Feldman, M.F. (2018) Uncovering the mechanisms of *Acinetobacter baumannii* virulence. *Nat Rev Microbiol* **16**: 91–102.

Kalscheuer, R., Syson, K., Veeraraghavan, U., Weinrick, B., Biermann, K.E., Liu, Z., *et al*. (2010) Self-poisoning of *Mycobacterium tuberculosis* by targeting GlgE in an alpha-glucan pathway. *Nat Chem Biol* **6**: 376–384.

Kormish, J.D., and McGhee, J.D. (2005) The *C. elegans* lethal gut obstructed *gob-1* gene is trehalose-6-phosphate phosphatase. *Dev Biol* **287**: 35–47.

Korte, J., and Alber, M. (2016) Trehalose-6-phosphate mediated toxicity determines essentiality of OtsB2 in *Mycobacterium tuberculosis in vitro* and in mice. *PLoS Path* **12**: e1006043.

Kurth, D., Belfiore, C., Gorriti, M.F., Cortez, N., Farias, M.E., and Albarracín, V.H. (2015) Genomic and proteomic evidences unravel the UV-resistome of the poly-extremophile *Acinetobacter* sp. Ver3. *Front Microbiol* **6**: 328.

Lee, J.J., Lee, S.-K., Song, N., Nathan, T.O., Swarts, B.M., Eum, S.-Y., *et al*. (2019) Transient drug-tolerance and permanent drug-resistance rely on the trehalose-catalytic shift in *Mycobacterium tuberculosis*. *Nat Commun* **10**: 2928.

Lucidi, M., Runci, F., Rampioni, G., Frangipani, E., Leoni, L., and Visca, P. (2018) New shuttle vectors for gene cloning and expression in multidrug-resistant *Acinetobacter Species*. *Antimicrob Agents Chemother* **62**: e02480–e02417.

Lunn, J.E., Feil, R., Hendriks, J.H.M., Gibon, Y., Morcuende, R., Osuna, D., *et al*. (2006) Sugar-induced increases in trehalose 6-phosphate are correlated with redox activation of ADP-glucose pyrophosphorylase and higher rates of starch synthesis in *Arabidopsis thaliana*. *Biochem J* **397**: 139–148.

Martínez-Esparza, M., Martínez-Vicente, E., González-Párraga, P., Ros, J.M., García-Peñarrubia, P., and Argüelles, J.C. (2009) Role of trehalose-6P phosphatase (TPS2) in stress tolerance and resistance to macrophage killing in *Candida albicans*. *Int J Med Microbiol* **299**: 453–464.

Martins, L.O., and Santos, H. (1995) Accumulation of mannosylglycerate and di-myo-inositol-phosphate by *Pyrococcus furiosus* in response to salinity and temperature. *Appl Environ Microbiol* **61**: 3299–3303.

Neidle, E.L., and Ornston, L.N. (1986) Cloning and expression of *Acinetobacter calcoaceticus* catechol 1,2-dioxygenase structural gene *catA* in *Escherichia coli*. *J Bacteriol* **168**: 815–820.

Peleg, A.Y., Seifert, H., and Paterson, D.L. (2008) *Acinetobacter baumannii*: emergence of a successful pathogen. *Clin Microbiol Rev* **21**: 538–582.

Perez, F., Hujer, A.M., Hujer, K.M., Decker, B.K., Rather, P. N., and Bonomo, R.A. (2007) Global challenge of multidrug-resistant *Acinetobacter baumannii*. *Antimicrob Agents Chemother* **51**: 3471–3484.

Piper, P.W., and Lockheart, A. (1988) A temperature-sensitive mutant of *Sacchromyces cerevisiae* defective in the specific phosphatase of trehalose biosynthesis. *FEMS Microbiol Lett* **49**: 245–250.

Puttikamonkul, S., Willger, S.D., Grahl, N., Perfect, J.R., Movahed, N., Bothner, B., *et al*. (2010) Trehalose-6-phosphate phosphatase is required for cell wall integrity and fungal virulence but not trehalose biosynthesis in the human fungal pathogen *Aspergillus fumigatus*. *Mol Microbiol* **77**: 891–911.

Ramirez, M.S., Penwell, W.F., Traglia, G.M., Zimbler, D.L., Gaddy, J.A., Nikolaidis, N., *et al*. (2019) Identification of potential virulence factors in the model strain *Acinetobacter baumannii A118*. *Front Microbiol* **10**: 1599.

Reina-Bueno, M., Argandoña, M., Nieto, J.J., Hidalgo-García, A., Iglesias-Guerra, F., Delgado, M.J., and Vargas, C. (2012) Role of trehalose in heat and desiccation tolerance in the soil bacterium *Rhizobium etli*. *BMC Microbiol* **12**: 207.

Rimmele, M., and Boos, W. (1994) Trehalose-6-phosphate hydrolase of *Escherichia coli*. *J Bacteriol* **176**: 5654–5664.

Roeßler, M., and Müller, V. (2001) Osmoadaptation in bacteria and archaea: common principles and differences. *Environ Microbiol* **3**: 743–754.

Runci, F., Gentile, V., Frangipani, E., Rampioni, G., Leoni, L., Lucidi, M., *et al*. (2019) Contribution of active iron uptake to *Acinetobacter baumannii* pathogenicity. *Infect Immun* **87**: e00755–e00718.

Sand, M., Mingote, A.I., Santos, H., Müller, V., and Averhoff, B. (2013) Mannitol, a compatible solute synthesized by *Acinetobacter baylyi* in a two-step pathway including a salt-induced and salt-dependent mannitol-1-phosphate dehydrogenase. *Environ Microbiol* **15**: 2187–2197.

Sand, M., de Berardinis, V., Mingote, A., Santos, H., Göttig, S., Müller, V., and Averhoff, B. (2011) Salt adaptation in *Acinetobacter baylyi*: identification and characterization of a secondary glycine betaine transporter. *Arch Microbiol* **193**: 723–730.

Schleucher, J., Schwendinger, M., Sattler, M., Schmidt, P., Schedletzky, O., Glaser, S.J., *et al*. (1994) A general enhancement scheme in heteronuclear multidimensional NMR employing pulsed field gradients. *J Biomol NMR* **4**: 301–306.

Scholz, A., Stahl, J., de Berardinis, V., Müller, V., and Averhoff, B. (2016) Osmotic stress response in *Acinetobacter baylyi*: identification of a glycine–betaine biosynthesis pathway and regulation of osmoadaptive choline uptake and glycine–betaine synthesis through a choline-responsive BetI repressor. *Environ Microbiol Rep* **8**: 316–322.

Singh, J.K., Adams, F.G., and Brown, M.H. (2019) Diversity and function of capsular polysaccharide in *Acinetobacter baumannii*. *Front Microbiol* **9**: 3301–3301.

Stahl, J., Bergmann, H., Göttig, S., Ebersberger, I., and Averhoff, B. (2015) *Acinetobacter baumannii* virulence is mediated by the concerted action of three phospholipases D. *PLoS One* **10**: e0138360.

Stainer, R.Y., and Ornston, L.N. (1973) The β-Ketoadipate pathway. *Adv Microb Physiol*, **9**: 89–151.

Thammahong, A., Puttikamonkul, S., Perfect, J.R., Brennan, R.G., and Cramer, R.A. (2017) Central role of the trehalose biosynthesis pathway in the pathogenesis of human fungal infections: opportunities and challenges for therapeutic development. *Microbiol Mol Biol Rev* **81**: e00053–e00016.

Tucker, A.T., Nowicki, E.M., Boll, J.M., Knauf, G.A., Burdis, N.C., Trent, M.S., and Davies, B.W. (2014) Defining gene-phenotype relationships in *Acinetobacter baumannii* through one-step chromosomal gene inactivation. *MBio* **5**: e01313–e01314.

van Vaeck, C., Wera, S., van Dijck, P., and Thevelein, J.M. (2001) Analysis and modification of trehalose 6-phosphate levels in the yeast *Saccharomyces cerevisiae* with the use of *Bacillus subtilis* phosphotrehalase. *Biochem J* **353**: 157–162.

Vicente, R.L., Spina, L., Gómez, J.P.L., Dejean, S., Parrou, J.-L., and François, J.M. (2018) Trehalose-6-phosphate promotes fermentation and glucose repression in *Saccharomyces cerevisiae*. *Microb Cell* **5**: 444–459.

Vriezen, J.A., de Bruijn, F.J., and Nüsslein, K. (2007) Responses of *Rhizobia* to desiccation in relation to osmotic stress, oxygen, and temperature. *Appl Environ Microbiol* **73**: 3451–3459.

Weidensdorfer, M., Ishikawa, M., Hori, K., Linke, D., Djahanschiri, B., Iruegas, R., *et al*. (2019) The Acinetobacter trimeric autotransporter adhesin Ata controls key virulence traits of *Acinetobacter baumannii*. *Virulence* **10**: 68–81.

Welsh, D.T., and Herbert, R.A. (1999) Osmotically induced intracellular trehalose, but not glycine betaine accumulation promotes desiccation tolerance in *Escherichia coli*. *FEMS Microbiol Lett* **174**: 57–63.

World Health Organization. (2017) Global priority list of antibiotic-resistant bacteria to guide research, discovery, and development of new antibiotics. URL https://www.who.int/medicines/publications/WHO-PPL-Short_Summary_25Feb-ET_NM_WHO.pdf.

Zaragoza, O., Blazquez, M.A., and Gancedo, C. (1998) Disruption of the *Candida albicans* TPS1 gene encoding trehalose-6-phosphate synthase impairs formation of hyphae and decreases infectivity. *J Bacteriol* **180**: 3809–3815.

Zeidler, S., and Müller, V. (2019a) Coping with low water activities and osmotic stress in *Acinetobacter baumannii*: significance, current status and perspectives. *Environ Microbiol* **21**: 2212–2230.

Zeidler, S., and Müller, V. (2019b) The role of compatible solutes in desiccation resistance of *Acinetobacter baumannii*. *Microbiology* **8**: e00740.

Zeidler, S., Hubloher, J., Schabacker, K., Lamosa, P., Santos, H., and Müller, V. (2017) Trehalose, a temperature- and salt-induced solute with implications in pathobiology of *Acinetobacter baumannii*. *Environ Microbiol* **19**: 5088–5099.

Zeidler, S., Hubloher, J., König, P., Ngu, N.D., Scholz, A., Averhoff, B., and Müller, V. (2018) Salt induction and activation of MtlD, the key enzyme in the synthesis of the compatible solute mannitol in *Acinetobacter baumannii*. *Microbiology* **7**: e00614.

Supporting Information

Additional Supporting Information may be found in the online version of this article at the publisher's web-site:

Table S1 Supplementary Information.